The Veterinary Journal 278 (2021) 105773

Contents lists available at ScienceDirect

The Veterinary Journal

journal homepage: www.elsevier.com/locate/tvjl

Computed tomography features for differentiating malignant and benign focal liver lesions in dogs: A meta-analysis

S. Burti, A. Zotti, B. Contiero, T. Banzato *

Department of Animal Medicine, Production and Health, University of Padua, Viale dell'Università 16, 35020 Legnaro, Padua, Italy

ARTICLE INFO

Keywords:
Diagnostic imaging
Evidence-based medicine
Liver
Meta-analysis

ABSTRACT

Computed tomography (CT) is often performed to complement ultrasound following detection of focal liver lesions (FLL). There is no consensus in the literature regarding the CT features that might be helpful in the distinction between benign and malignant FLL. The aim of this meta-analysis was to identify, based on the available literature, the qualitative and quantitative CT features able to distinguish between benign and malignant FLL. Studies on the diagnostic accuracy of CT in characterising FLL were searched in MEDLINE, Web of Science, and Scopus databases. Pooled sensitivity, pooled specificity, diagnostic odds ratio (DOR), receiver operator curve (ROC) area, were calculated for qualitative features. DOR were used to determine which qualitative features were most informative to detect malignancy; quantitative features were selected/identified based on standardised mean difference (SMD).

Well-defined margins, presence of a capsule, abnormal lymph nodes, and heterogeneity in the arterial, portal and delayed phase were classified as informative qualitative CT features. The pooled sensitivity ranged from 0.630 (abnormal lymph nodes) to 0.786 (well-defined margins), while pooled specificity ranged from 0.643 (well-defined margins) to 0.816 (heterogeneous in delayed phase). Maximum dimensions, ellipsoid volume, attenuation of the liver in the pre-contrast phase, and attenuation of the liver in the arterial, portal, and delayed phase were found to be informative quantitative CT features. Larger maximum dimensions and volume (positive SMD), and lower attenuation values (negative SMD) were more associated with malignancy. This meta-analysis provides the evidence base for the interpreting CT imaging in the characterization of FLL.

Introduction

Computed tomography (CT) is widely used for the diagnosis and monitoring of many diseases in dogs. CT is also frequently used as a stand-alone diagnostic imaging technique for neoplasm staging. Masses or nodules may also be found incidentally during CT imaging performed to investigate diseases elsewhere in the body (Burti et al., 2021). Regardless of reason for scanning, focal liver lesions (FLL) are common findings on CT scans of dogs, especially when older animals are investigated (Jones et al., 2016). FLL may also be initially identified using other diagnostic imaging techniques, such as ultrasonography, and then, if appropriate, better characterised by means of CT (Marolf, 2017). CT offers the ability to evaluate the liver and any lesions in three dimensions and provides superior visualisation of lesional vascularisation in comparison to ultrasound. Furthermore, some types of lesion (e.g. vacuolar degeneration) are detectable only through enhanced CT techniques. While the CT features of the different histotypes of FLL have been widely investigated in human medicine, and, especially in the case of hepatocellular carcinoma (HCC; Shah et al., 2014), are well known and characterised (Ariff et al., 2009; Chou et al., 2015); to date, the CT features of FLL in dogs have been infrequently described. In addition, although some features (e.g., enhancement in the delayed phase, lesion dimensions) have been reported as useful in differentiating between benign and malignant FLL in dogs (Griebie et al., 2017; Burti et al., 2021), other authors report that no CT features were useful to aid this differentiation (Stehlík et al., 2020). The usefulness of CT in discriminating between benign and malignant FLL is still to be fully determined.

The aim of this meta-analysis was to identify qualitative and quantitative CT features useful in distinguishing between benign and malignant FLL and to summarise their diagnostic accuracy.

Materials and methods

This meta-analysis was performed in accordance with the best

* Corresponding author.
E-mail address: tommaso.banzato@unipd.it (T. Banzato).

https://doi.org/10.1016/j.tvjl.2021.105773

Available online 3 November 2021

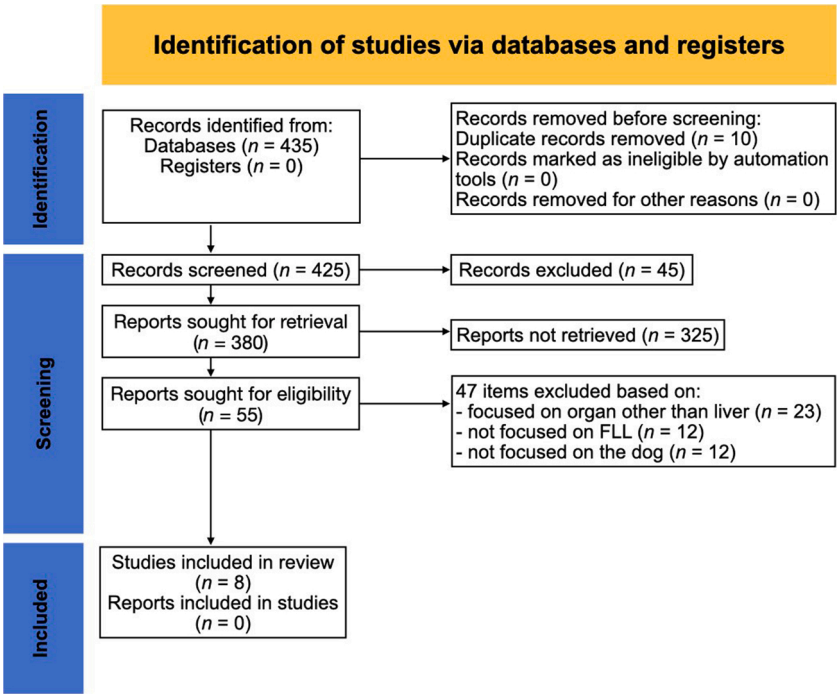

Fig. 1. Flow chart showing the literature search process.

Table 1
Characteristics of the studies included in the analysis.

Reference	Study design / Country	Time period	Scanning method	Dogs / FLL (*n*)	Age range (years)	Body weight (kg)	Diagnosis (*n*)	Lesion size (cm)
Stehlik et al. (2020)	Retrospective / Czech Republic and Italy	2016–2019	Triple-phase CT	3	5–16 years	23.3 ± 10.8[a]	Benign (17) Malignant (14)	
Burti et al. (2021)	Retrospective/ Italy	2015–2020	Dual-phase CT	69	4–16 years	Not given	Benign (37) Malignant (32)	5.37 ± 4.36[a]
Leela-Arporn et al. (2019)	Prospective/ Japan	2016–2019fl	Triple-phase CT	57 / 70	8–13 years	9.2 ± 6.6[a]	Benign (18) Malignant (52)	4.85 ± 2.25[a,c]
Griebie et al. (2017)	Retrospective/ USA	2014–2016	Triple-phase CT	44 / 46	4–13 years	Not given	Benign (16) Malignant (30)	7.135[c]
Jones et al. (2016)	Retrospective/ UK	2008–2014	Dual-phase CT	24	3–15 years	24 (4–54)[b]	Benign (10) Malignant (14)	6.0 (1.5–6.95)[b]
Kutara et al. (2014)	Prospective / Japan	Not given	Triple-phase CT	70	7–16 years	14.8 ± 9.1[a]	Benign (14) Malignant (56)	6.35 ± 3.32[a]
Fukushima et al. (2012)	Retrospective/ Japan	2005–2010	Triple-phase CT	33	0.25–15 years	7.2 (1.5–38.5)[b]	Benign (19) Malignant (14)	7.77 (2.8–16.5)[b,c]
Taniura et al. (2009)	Retrospective/ Japan	2004–2007	Triple-phase CT	76	Not given	Not given	Benign (40) Malignant (36)	4.76 ± 2.06[a,c]

CT, computed tomography; FLL, focal liver lesions.
[a] Mean (± standard deviation).
[b] Median (range).
[c] Pooled results from available data.

Table 2
Risk of bias and applicability concerns assessment for each of the studies included in the analysis.

Reference	Risk of bias				Applicability concerns		
	Case selection	Index test	Reference standard	Flow and timing	Case selection	Index test	Reference standard
Taniura et al. (2009)	High	Unknown	Unknown	Low	High	Unknown	Unknown
Fukushima et al. (2012)	Low	Low	Unknown	Low	Low	Low	Low
Kutara et al. (2014)	High	Unknown	Unknown	Low	High	Unknown	Low
Jones et al. (2016)	Low	Low	Unknown	Low	Low	Low	Low
Griebie et al. (2017)	Low	Low	Unknown	Low	Low	Low	Low
Leela-Arporn et al. (2019)	Low	Low	Unknown	Low	Low	Low	Low
Stehlik et al. (2020)	Low	Low	Unknown	Low	Low	Low	Low
Burti et al., 2021	Low	Low	Unknown	Low	Low	Low	Low

practices in diagnostic test accuracy systematic reviews (PRISMA-DATA; Moher et al., 2009; DerSimonian and Laird, 2015).

Search strategy

A literature search was conducted based on the PICOS (population, intervention, comparator, outcome, study design) approach (Methley et al., 2014). The target population was dogs with FLL evident on CT scans that had histopathological analysis of the FLL performed. Intervention was identification of CT features. Outcome was the diagnostic accuracy on benign vs. malignant characterisation of the FLL. FLL were defined as liver nodule(s) or mass(es) of any dimensional value, that were identified in the CT scans due to their different attenuation when compared to the surrounding liver parenchyma. Study design was controlled or comparative, randomised or non-randomised experimental studies, or prospective or retrospective observational studies. A search of the MEDLINE, Web of Science, and Scopus databases from January 2000 to Jan 2021 was performed. To maximise inclusion of articles for review, we opted to perform a search based on generic terms. Keywords used for searching were (computed tomography OR "CT" AND liver OR hepatic AND dog OR canine). The literature search was restricted to articles written in the English language.

Screening of studies

Screening of the studies was performed by two authors. The studies were first screened at both title and abstract level. Reviews were excluded. Thereafter, the identified articles were selected at a full-text level and only those that entirely met the PICOS criteria were included.

Eligibility criteria

The inclusion criteria for the studies were: (1) CT evaluation of FLL in dogs; (2) evaluation of qualitative and quantitative CT features; (3) cytological and/or histological diagnosis of the lesions.

Reference standard

The reference standard were lesions with cytological and/or histological-confirmed diagnosis. Studies that used either histopathology and/or cytology as reference standards were included. Reference standards that fulfilled the above criteria were considered at low risk of bias.

Data extraction

For each included study, the following characteristics were recorded: type of study (i.e. prospective or retrospective), country in which the study was performed, time period over which data were collected, CT scanning method (i.e. dual-phase or triple-phase), number of dogs or FLL, age, body weight, and FLL size. In addition, the cytopathological/histopathological categories used, along with the number of FLL within each category, were also recorded. The cytopathological/histopathological categories used were condensed into 'benign' (which included nodular hyperplasia [NH]) or 'malignant' (which included HCC).

Risk of bias assessment

The risk of bias was assessed using the QUADAS-2 tool (Whiting et al., 2011). No modification to this tool was necessary for the specific search question. The assessment was completed independently by two authors. Discrepancies were resolved with the aid of a co-author of this study.

Outcomes

The primary outcome was the sensitivity and specificity of individual CT features in the identification of malignant FLL in dogs. Data were analysed on a per-lesion level, as both benign and malignant lesions can be present in the same individual at the same time. Secondary outcomes were CT characteristics, study population factors, study design, and risk of bias.

Data analysis

For dichotomous predictor variables, diagnostic test measures were calculated using 2 × 2 contingency tables based on the number of FLL displaying each CT feature as reported in the results of the articles included in the meta-analysis. Sensitivity, specificity, and accuracy, along with their 95% confidence intervals (CI), were calculated for each individual study. The area under the receiver operating characteristic (ROC) curves (AUC) was also estimated, and this information was used for meta-analysis of the qualitative features. The outcome of the meta-analysis was a pooled estimate of sensitivity, specificity, diagnostic odds ratio (DOR), and AUC. Based on these aggregated results, it was possible to determine whether the presence of a certain CT feature was an accurate predictor for malignancy. DOR could range from 0 to infinity, with higher values indicating better discriminatory test performance. As value of 1 implies that the test had no discriminative power, any CT feature where the 95% CI of its DOR did not span 1 was

Table 3
Calculated accuracy measures of malignant diagnosis considering the qualitative features.

Qualitative feature and references	Sensitivity (95% CI)	Specificity (95% CI)	Accuracy (95% CI)	Area under the curve	SE
Well-defined margins					
Burti et al. (2021)	0.750 (0.566–0.885)	0.487 (0.319–0.656)	0.608 (0.483–0.724)	0.618	0.070
Leela-Arporn et al. (2019)	0.933 (0.841–0.988)	0.933 (0.173–0.643)	0.800 (0.687–0.886)	0.666	0.070
Jones et al. (2016)	0.500 (0.230–0.700)	0.600 (0.262–0.878)	0.542 (0.328–0.745)	0.550	0.120
Fukushima et al. (2012)	0.857 (0.572–0.982)	0.211 (0.061–0.456)	0.485 (0.308–0.665)	0.534	0.100
Taniura et al. (2009)	0.694 (0.519–0.837)	1 (0.912–1)	0.855 (0.756–0.926)	0.847	0.040
Irregular surface					
Burti et al. (2021)	0.938 (0.792–0.992)	0.432 (0.271–0.605)	0.667 (0.543–0.776)	0.685	0.060
Leela-Arporn et al. (2019)	0.346 (0.220–0.491)	0.940 (0.727–0.999)	0.500 (0.378–0.622)	0.645	0.070
Fukushima et al. (2012)	0.571 (0.289–0.823)	0.211 (0.061–0.456)	0.364 (0.204–0.549)	0.527	0.100
Presence of a capsule					
Burti et al. (2021)	0.500 (0.319–0.681)	0.811 (0.648–0.920)	0.667 (0.543–0.776)	0.655	0.070
Leela-Arporn et al. (2019)	0.423 (0.287–0.568)	0.889 (0.653–0.986)	0.543 (0.419–0.663)	0.656	0.070
Fukushima et al. (2012)	0.929 (0.661–0.998)	0.474 (0.245–0.711)	0.667 (0.482–0.820)	0.701	0.090
Taniura et al. (2009)	0.694 (0.519–0.837)	1 (0.912–1)	0.855 (0.756–0.926)	0.847	0.050
Abnormal lymph nodes					
Burti et al. (2021)		0.838 (0.680–0.938)	0.710 (0.588–0.813)	0.700	0.060
Jones et al. (2016)	0.785 (0.492–0.953)	0.400 (0.122–0.738)	0.625 (0.406–0.812)	0.593	0.120
Marginal enhancement pattern					
Burti et al. (2021)	0.156 (0.053–0.328)	0.811 (0.648–0.920)	0.507 (0.384–0.630)	0.484	0.070
Jones et al. (2016)	0.143 (0.018–0.428)	0.800 (0.444–0.975)	0.417 (0.221–0.634)	0.471	0.120
Diffuse enhancement pattern					
Burti et al. (2021)	0.813 (0.636–0.928)	0.189 (0.080–0.352)	0.478 (0.357–0.602)	0.501	0.070
Jones et al. (2016)	0.857 (0.572–0.982)	0.200 (0.025–0.556)	0.583 (0.366–0.779)	0.529	0.120
Hypoattenuation					
Burti et al. (2021)	0.875 (0.710–0.965)	0.243 (0.118–0.412)	0.536 (0.412–0.657)	0.559	0.060
Taniura et al. (2009)	0.833 (0.672–0.936)	0.850 (0.702–0.943)	0.842 (0.740–0.916)	0.842	0.040
Heterogeneous in arterial phase					
Leela-Arporn et al. (2019)	0.769 (0.632–0.875)	0.556 (0.308–0.785)	0.714 (0.594–0.816)	0.662	0.100
Kutara et al. (2014)	0.714 (0.578–0.827)	0.571 (0.289–0.823)	0.686 (0.564–0.792)	0.643	0.110
Heterogeneous in portal phase					
Burti et al. (2021)	0.813 (0.636–0.928)	0.514 (0.344–0.681)	0.652 (0.528–0.763)	0.663	0.070
Leela-Arporn et al. (2019)	0.769 (0.632–0.875)	0.722 (0.465–0.903)	0.757 (0.640–0.852)	0.746	0.060
Jones et al. (2016)	0.429 (0.177–0.711)	0.400 (0.122–0.738)	0.417 (0.221–0.634)	0.714	0.100
Kutara et al. (2014)	0.714 (0.578–0.827)	0.929 (0.661–0.998)	0.757 (0.640–0.852)	0.821	0.050
Heterogeneous in delayed phase					
Leela-Arporn et al. (2019)	0.750 (0.611–0.860)	0.722 (0.465–0.903)	0.743 (0.624–0.840)	0.736	0.060
Kutara et al. (2014)	0.554 (0.415–0.687)	0.929 (0.661–0.998)	0.629 (0.505–0.741)	0.741	0.070
Enhancement in portal phase – HYPO					
Stehlik et al. (2020)	0.429 (0.177–0.711)	0.412 (0.184–0.671)	0.419 (0.246–0.609)	0.420	0.100
Leela-Arporn et al. (2019)	0.096 (0.032–0.210)	0.833 (0.586–0.964)	0.286 (0.184–0.406)	0.465	0.080
Jones et al. (2016)	0.143 (0.018–0.428)	0.800 (0.444–0.975)	0.417 (0.221–0.634)	0.471	0.120
Kutara et al. (2014)	0.571 (0.432–0.703)	1 (0.768–1)	0.657 (0.534–0.766)	0.786	0.060
Fukushima et al. (2012)	0.857 (0.572–0.982)	0.421 (0.203–0.665)	0.606 (0.421–0.771)	0.639	0.100
Taniura et al. (2009)	0.917 (0.775–0.983)	0.975 (0.868–0.999)	0.947 (0.871–0.986)	0.946	0.030
Enhancement in portal phase – ISO					
Stehlik et al. (2020)	0.571 (0.289–0.823)	0.706 (0.440–0.897)	0.645 (0.454–0.808)	0.639	0.100
Leela-Arporn et al. (2019)	0.154 (0.069–0.281)	0.778 (0.524–0.936)	0.314 (0.209–0.436)	0.466	0.080
Kutara et al. (2014)	0.268 (0.158–0.403)	0.643 (0.351–0.872)	0.343 (0.234–0.466)	0.455	0.090
Fukushima et al. (2012)	0.143 (0.018–0.428)	0.842 (0.604–0.966)	0.546 (0.364–0.719)	0.492	0.100
Taniura et al. (2009)	0.056 (0.068–0.187)	0.075 (0.016–0.204)	0.066 (0.022–0.147)	0.065	0.030
Enhancement in portal phase – HYPER					
Stehlik et al. (2020)	0 (0–0.232)	0.882 (0.636–0.985)	0.484 (0.301–0.669)	0.441	0.100
Leela-Arporn et al. (2019)	0.750 (0.611–0.860)	0.389 (0.173–0.643)	0.657 (0.534–0.767)	0.569	0.080
Jones et al. (2016)	0.500 (0.230–0.770)	0.900 (0.555–0.998)	0.667 (0.447–0.844)	0.700	0.110
Kutara et al. (2014)	0.161 (0.076–0.283)	0.357 (0.128–0.649)	0.200 (0.114–0.313)	0.259	0.080
Fukushima et al. (2012)	0 (0–0.232)	0.737 (0.488–0.909)	0.424 (0.255–0.608)	0.368	0.100
Taniura et al. (2009)	0.028 (0–0.145)	1 (0.912–1)	0.539 (0.421–0.654)	0.514	0.070
Enhancement in delayed phase – HYPO					
Stehlik et al. (2020)	0.357 (0.128–0.649)	0.529 (0.278–0.770)	0.452 (0.273–0.640)	0.443	0.110
Burti et al. (2021)	0.906 (0.750–0.980)	0.162 (0.062–0.320)	0.507 (0.384–0.630)	0.534	0.070
Leela-Arporn et al. (2019)	0.039 (0.005–0.132)	0.833 (0.586–0.964)	0.243 (0.148–0.360)	0.436	0.080
Kutara et al. (2014)	0.482 (0.347–0.620)	1 (0.768–1)	0.586 (0.462–0.702)	0.741	0.070
Fukushima et al. (2012)	0.929 (0.661–0.998)	0.421 (0.202–0.665)	0.636 (0.451–0.796)	0.675	0.100
Taniura et al. (2009)	0.944 (0.813–0.993)	1 (0.912–1)	0.974 (0.908–0.997)	0.972	0.020
Enhancement in delayed phase – ISO					
Stehlik et al. (2020)	0.571 (0.289–0.823)	0.471 (0.229–0.722)	0.516 (0.331–0.699)	0.521	0.110
Burti et al. (2021)	0 (0–0.109)	0.973 (0.858–0.999)	0.522 (0.384–0.630)	0.486	0.070
Leela-Arporn et al. (2019)	0.308 (0.187–0.451)	0.556 (0.308–0.785)	0.371 (0.259–0.495)	0.432	0.080
Kutara et al. (2014)	0.393 (0.265–0.533)	0.286 (0.084–0.581)	0.371 (0.259–0.495)	0.339	0.090
Fukushima et al. (2012)	0.071 (0.002–0.339)	0.632 (0.384–0.837)	0.394 (0.229–0.579)	0.352	0.100
Taniura et al. (2009)	0.056 (0.007–0.187)	0 (0–0.088)	0.026 (0.003–0.092)	0.028	0.020
Enhancement in delayed phase – HYPER					
Stehlik et al. (2020)	0.071 (0.002–0.339)	1 (0.805–1)	0.581 (0.391–0.754)	0.536	0.110

(*continued on next page*)

Table 3 (*continued*)

Qualitative feature and references	Sensitivity (95% CI)	Specificity (95% CI)	Accuracy (95% CI)	Area under the curve	SE
Burti et al. (2021)	0.062 (0.008–0.208)	0.865 (0.712–0.955)	0.493 (0.370–0.616)	0.464	0.070
Leela-Arporn et al. (2019)	0.654 (0.509–0.780)	0.611 (0.358–0.827)	0.643 (0.519–0.754)	0.632	0.070
Kutara et al. (2014)	0.125 (0.052–0.241)	0.714 (0.419–0.916)	0.243 (0.148–0.360)	0.420	0.090
Fukushima et al. (2012)	0 (0–0.232)	0.947 (0.740–0.999)	0.546 (0.363–0.719)	0.474	0.100

95% CI, 95% confidence interval; SE, standard error;

considered as informative.

For the continuous predictors, the descriptive statistics (as mean and standard deviation (SD); or median and range) were reported for the two groups (malignant vs. benign) as reported in their respective individual studies. For the meta-analysis of the continuous measures, comparison of the means between malignant and benign cases was performed using the standardised mean difference (SMD). For the studies reporting only the range the SD was estimated by dividing the range by 4. Based on the pooled result, any CT features where the 95% CI of its SMD did not span 0 were considered statistically significant at the 5% level ($P < 0.05$). Cohen's rule of thumb for interpreting the SMD statistic is to consider the absolute value: a value of 0.2 indicates a small effect, a value of 0.5 indicates a medium effect and a value of 0.8 or higher indicates a large effect.

For both qualitative and quantitative CT features, study heterogeneity was assessed to determine whether a fixed or random effects model had to be used for the meta-analysis. The agreement or disagreement between the studies was examined using different measures of heterogeneity: Cochran's Q and I^2 statistics (Higgins, 2003). A $Q > 0.1$ and an $I^2 > 0.5$ were considered as indicative for heterogeneity. When heterogeneity was present, the random effects model was used.

Forest plot graphs were used to show the meta-analysis results for every study, along with the 95% CI and the numerical estimate of the overall effect of interest (global DOR or SMD, sensitivity, and specificity). In the graphs, the length of the horizontal lines represents the confidence intervals of the studies, the dimensions of the boxes represent the weights assigned to each of them. These weights depended on sample size and on the model adopted (fixed or random effects). All the analyses were conducted using 'mada' (Doebler, 2020, URL http://CRAN.R-project.org/package= mada. R package version 0.5 7 (5), 2016) and 'meta' (Schwarzer, 2021, https://cran.r-project.org/web/packages/meta/meta.pdf) packages (Shim et al., 2019) of R (version: 2020)[1] .

Results

Study search

The search in the MEDLINE, Web of Science, and Scopus databases retrieved 435 potentially relevant studies. Duplicates were removed. All the articles not matching the inclusion criteria (case reports, reviews, letters, abstracts, recommendations, guidelines) were excluded (n = 427). Eight articles in total matched the inclusion criteria. The study selection process is reported in Fig. 1.

Study characteristics

A total of 404 dogs were included, and the CT features of 419 FLL, along with their histopathological or cytological diagnosis, were reported. In Taniura et al. (2009) only FLL with a diagnosis of nodular hyperplasia (NH) or HCC were included. In Fukushima et al. (2012) only FLL with a diagnosis of HCC, NH, or another benign process were included. No a-priori selection of the FLL was made in the remaining studies. The characteristics of the studies are summarised in Table 1.

Quality of the studies

The risk of bias was evaluated as high for the selection of cases in the studies by Taniura et al. (2009) and Kutara et al. (2014), as only dogs diagnosed with certain pathologies (NH and HCC in Taniura et al., 2009; HCC, NH and metastatic tumours in Kutara et al., 2014) were included. The applicability of the results presented, as well as the applicability of the index test, were consequentially considered as heavily biased. For the remaining studies the risk of bias was classified as low for: case selection, Index test, and flow and timing. For all the studies, the blinding of pathologists and radiologists to the results of other tests was not mentioned and, therefore, classified as unknown. Lastly, a power analysis was not conducted in any of the included studies. The study quality results are summarised in Table 2.

Categorisation of the CT features

Twenty-eight overlapping CT features were evaluated in the different studies. Sixteen qualitative features (well-defined margins, irregular surface, presence of a capsule, abnormal lymph nodes, marginal enhancement pattern, diffuse enhancement pattern, heterogeneous pattern in arterial phase, heterogeneous pattern in portal phase, heterogeneous pattern in delayed phase, hypoattenuation, and hypoenhancement, enhancement in the portal phase, and enhancement in the delayed phase; these latter two features were further divided into hypo, iso, and hyper) and 10 quantitative continuous features (maximum dimension, ellipsoid volume, attenuation of normal liver in the pre-contrast phase, attenuation of normal liver in arterial phase, attenuation of normal liver in portal phase, attenuation of normal liver in delayed phase, attenuation of pre-contrast FLL, attenuation of FLL in arterial phase, attenuation of FLL in portal phase, attenuation of FLL in delayed phase) were considered because these were evaluated in at least two studies.

Diagnostic accuracy of the CT features in the individual studies

The sensitivity, specificity, accuracy, and AUC of the qualitative CT features as evaluated in each study are reported in Table 3. The mean and the standard deviation and/or median with overall range of the continuous variables as evaluated in the individual studies are reported in Table 4. Taniura et al. (2009) reported AUCs above 0.80 for most of the considered CT features, whereas Kutara et al. (2014) reported an AUC of 0.82 for heterogeneity in the portal phase. Accuracy index values higher than 80% were evident for well-defined margins in (Leela-Arporn et al., 2019) and Taniura et al. (2009), and for presence of a capsule, hypoattenuation, and hypoenhancement in the portal phase and delayed phase in Taniura et al. (2009). Significant differences for the quantitative CT features were reported for the maximum lesion dimensions in (Leela-Arporn et al., 2019) and Taniura et al. (2009), for attenuation of pre-contrast normal liver in Burti et al. (2021), and for ellipsoid volume, attenuation of post-contrast normal liver, and attenuation of normal liver in portal phase in (Leela-Arporn et al., 2019).

[1] See: R: A Language and Environment for Statistical Computing https://www.R-project.org (Accessed 25 October 2021).

Table 4
Descriptive values for malignant and benign lesions recorded as quantitative continuous features with reported *P*-values.

Qualitative feature and references	Malignant	Benign	Reported *P*-value
Maximum dimension (cm)			
Burti et al. (2021)	4.3 (0.5–16.3)	3.5 (0.5–18.1)	0.06
Leela-Arporn et al. (2019)	6.6 (±3.1)	3.1 (±1.4)	<0.0001
Jones et al. (2016)	6.1 (1.5–69.5)	6.0 (3.2–34.5)	0.95
Taniura et al. (2009)	6.8 (±3.5)	2.7 (±0.6)	<0.05
Ellipsoid volume (cm^3)			
Burti et al. (2021)	20.8 (0.02–1576)	11.5 (0.04–1995)	0.20
Leela-Arporn et al. (2019)	195.0 (±228.6)	21.3 (±24.5)	<0.0001
Attenuation of pre-contrast normal liver (HU)			
Stehlik et al. (2020)	63.1 (±9.0)	60.9 (±8.7)	n.s.
Burti et al. (2021)	58.9 (46.2–82.1)	66.1 (51.8–85.5)	< 0.01
Jones et al. (2016)	60.0 (53.0–75.0)	71.0 (49.0–79.0)	0.13
Taniura et al. (2009)	58.1 (±11.2)	62.7 (±8.1)	Not reported
Attenuation of pre-contrast lesion (HU)			
Burti et al. (2021)	40.3 (10.5–67.3)	43.7 (9.6–70.1)	0.66
Jones et al. (2016)	46.0 (32.0–68.0)	60.0 (26.0–69.0)	0.32
Taniura et al. (2009)	44.2 (±11.6)	61.1 (±10.1)	Not reported
Attenuation of arterial phase – normal liver (HU)			
Stehlik et al. (2020)	67.9 (±7.1)	69.9 (±16.1)	n.s.
Leela-Arporn et al. (2019)	117.2 (±18.4)	121.2 (±16.1)	0.39
Taniura et al. (2009)	106.1 (±26.4)	111.9 (±24.8)	Not reported
Attenuation of arterial phase – lesion (HU)			
Stehlik et al. (2020)	52.8 (±17.2)	65.0 (±28.8)	n.s.
Leela-Arporn et al. (2019)	112.0 (±49.6)	134.7 (±72.3)	0.15
Taniura et al. (2009)	91.1 (±35.2)	116.1 (±44.4)	Not reported
Attenuation of portal phase – normal liver (HU)			
Stehlik et al. (2020)	113.8 (±11.4)	114.6 (±18.7)	n.s.
Leela-Arporn et al. (2019)	156.0 (±25.5)	172.1 (±26.3)	0.03
Taniura et al. (2009)	136.6 (±23.7)	126.0 (±21.8)	Not reported
Attenuation of portal phase – lesion (HU)			
Stehlik et al. (2020)	85.6 (±30.6)	90.5 (±42.4)	n.s.
Leela-Arporn et al. (2019)	118.4 (±44.9)	148.4 (±61.1)	0.07
Taniura et al. (2009)	109.8 (±38.9)	130.8 (±24.3)	Not reported
Attenuation of delayed phase – normal liver (HU)			
Stehlik et al. (2020)	107.1 (±13.2)	112.8 (±7.1)	n.s.
Leela-Arporn et al. (2019)	125.3 (±16.8)	131.1 (±15.4)	0.19
Taniura et al. (2009)	127.7 (±22.1)	122.9 (±17.7)	Not reported
Attenuation of delayed phase – lesion (HU)			
Stehlik et al. (2020)	87.0 (±30.2)	83.2 (±29.3)	n.s.
Burti et al. (2021)	83.2 (62.4–121.2)	83.9 (62.6–121.3)	0.13
Leela-Arporn et al. (2019)	105.2 (± 28.1)	119.7 (± 37.5)	0.15
Jones et al. (2016)	77.0 (42.0–120.0)	99.0 (25.0–121.0)	0.62
Taniura et al. (2009)	104.9 (±34.6)	123.9 (±17.5)	Not reported

n.s., Reported as not statistically significant ($P > 0.05$); HU, Hounsfield unit; CE, contrast-enhanced.
[a]Data are reported as mean (± standard deviation) or as median (range);

Overall diagnostic accuracy

Results of the meta-analysis for qualitative CT features reported in at least two studies are reported in Table 5. The pooled sensitivity, specificity, DOR, and AUC were calculated using either a fixed or random effects model, depending on the outcome of the heterogeneity test. The results of the heterogeneity tests for each variable considered are reported as Supplementary Material. Six of the 16 qualitative features included in the meta-analysis were considered as informative. These were: well-defined margins, presence of a capsule, abnormal lymph nodes, and heterogeneity in the arterial, portal, and delayed phase. Of these, presence of a capsule and hyperenhancement in the delayed phase showed the highest specificity, with 0.884 (95% CI 0.537–0.980) and 0.864 (95% CI 0.681–0.950) respectively. These results were considered quite robust, as they were based on four and five studies respectively. Two variables showed a pooled sensitivity above 0.8, these were: hypoattenuation (0.853, 95% CI 0.748–0.919) and diffuse enhancement pattern (0.826, 95% CI 0.689–0.911). However, these results were based on only two studies each, with hypoattenuation evaluated in Burti et al. (2021) and Taniura et al. (2009), and diffuse enhancement pattern evaluated in Burti et al. (2021) and Jones et al. (2016). Heterogeneity in the portal phase showed the highest overall diagnostic accuracy, with an AUC of 0.751 and a DOR of 4.749. The forest plots of the pooled diagnostic accuracy measures (sensitivity, specificity, and DOR) for heterogeneity in the portal phase is reported in Fig. 2. The remaining forest plots graphs are reported as Supplementary Material.

The results of the SMD test for quantitative features evaluated in at least two studies are reported in Table 6. Based on the SMD test, maximum dimension, ellipsoid volume, attenuation of pre-contrast liver, and attenuation of the liver in the arterial, portal, and delayed phase were considered informative. The SMD was negative for all informative quantitative CT features based on attenuation, meaning that malignant lesions showed lower attenuation values than benign lesions. Ellipsoid volume and the maximum dimension had positive SMD. Forest plots reporting the pooled SMD for the informative quantitative CT features are reported in Fig. 3.

Discussion

The results of this meta-analysis revealed that, based on the available literature, some qualitative CT features showed statistically significant differences between benign and malignant FLL. The presence of a capsule, hypoattenuation, and heterogeneity in the delayed phase showed the highest DOR and, therefore, are the most reliable qualitative CT features for the detection of malignant FLL. Well-defined margins, abnormal lymph nodes, heterogeneity in the arterial phase, and

Table 5
Summary of meta-analysis for qualitative features: diagnostic accuracy of the predictors to identify the malignant cases. Overall sensitivity, specificity, and diagnostic odd's ratio (DOR) are reported with 95% confidence interval between parentheses. Overall area under the curve (AUC) and standard error (SE) are reported.

CT features	Studies (*n*)	Sensitivity	Specificity	DOR	AUC	SE
Well-defined margins	5	0.790 (0.622–0.890)	0.641 (0.220–0.921)	4.83 (1.43–16.36)	0.677	0.06
Irregular surface	3	0.680 (0.291–0.922)	0.580 (0.163–0.909)	3.18 (0.30–33.29)	0.535	0.07
Capsule presence	4	0.631 (0.420–0.809)	0.883 (0.537–0.980)	9.61 (2.75–33.55)	0.728	0.05
Abnormal lymph nodes	2	0.633 (0.483–0.760)	0.678 (0.331–0.901)	5.02 (1.94–12.99)	0.676	0.06
Marginal enhancement pattern	2	0.151 (0.070–0.290)	0.806 (0.670–0.910)	0.76 (0.26–2.25)	0.481	0.06
Diffuse enhancement pattern	2	0.834 (0.692–0.914)	0.194 (0.103–0.332)	1.11 (0.39–3.19)	0.508	0.06
Hypoattenuation	2	0.850 (0.750–0.919)	0.571 (0.153–0.913)	8.04 (0.67–96.26)	0.708	0.10
Heterogeneous in arterial phase	2	0.740 (0.650–0.815)	0.523 (0.392–0.721)	3.75 (1.64–8.57)	0.654	0.07
Heterogeneous in portal phase	4	0.730 (0.653–0.792)	0.660 (0.431–0.831)	4.75 (1.16–19.42)	0.751	0.03
Heterogeneous in delayed phase	2	0.652 (0.511–0.780)	0.820 (0.610–0.930)	9.34 (3.28–26.61)	0.738	0.04
Enhancement in portal phase						
- Hypo-	6	0.510 (0.230–0.811)	0.831 (0.533–0.964)	4.22 (0.58–30.91)	0.640	0.08
- Iso-	5	0.200 (0.091–0.373)	0.599 (0.281–0.853)	0.37 (0.05–2.51)	0.407	0.09
- Hyper-	6	0.102 (0.011–0.503)	0.810 (0.480–0.950)	0.71 (0.14–3.61)	0.472	0.06
Enhancement in delayed phase						
- Hypo-	6	0.663 (0.243–0.921)	0.832 (0.313–0.984)	4.83 (0.66–35.32)	0.646	0.08
- Iso-	6	0.151 (0.043–0.423)	0.442 (0.091–0.869)	0.20 (0.05–0.83)	0.345	0.07
- Hyper-	5	0.110 (0.020–0.390)	0.861 (0.683–0.950)	0.93 (0.30–2.89)	0.511	0.04

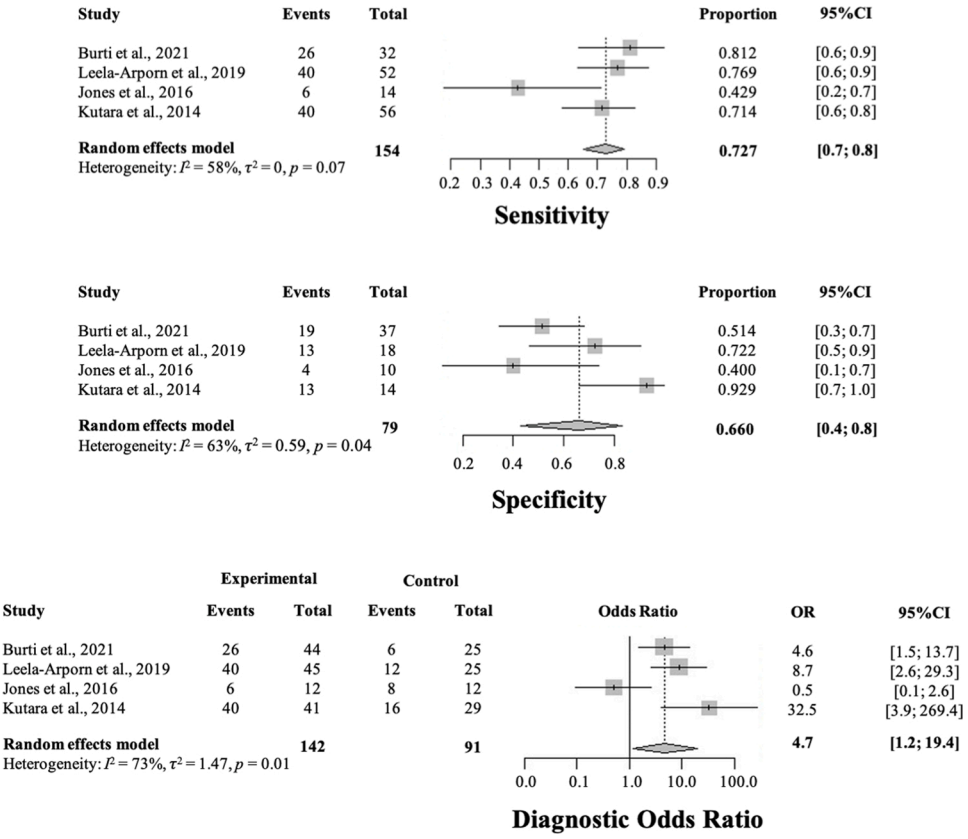

Fig. 2. Forest plot of the pooled diagnostic accuracy measures (sensitivity, specificity, and diagnostic odds ratio [DOR]) for heterogeneity in the portal phase. The squares represent the proportion of malignant focal liver lesion (FLL) and the whiskers represent the 95% confidence interval (CI). The diamond represents the pooled effect. The location of the diamond represents the estimated effect size, and the width of the diamond reflects the precision of the estimate. Heterogeneity indexed (I^2 and χ^2 = Q) were also reported.

heterogeneity in the portal phase were also found to be informative, albeit with a lower level of confidence. The quantitative features of maximal FLL dimension, attenuation of pre-contrast normal liver, and attenuation of the normal liver in the arterial, portal, and delayed phases had statistically significant differences between benign and malignant groups. Interestingly, the attenuation of the CT-normal liver parenchyma showed statistically significant differences between benign and malignant FLL. The finding of significant differences between attenuation of what was considered to be 'normal' liver between the two groups might indicate that the 'normal' liver parenchyma surrounding the malignant FLL could also be involved in the neoplastic process. This implies that, in addition to sampling the FLL, sampling of the 'normal' liver parenchyma should be considered.

As only individual CT features could be analysed in this meta-analysis, the overall accuracy of CT in the detection of malignant FLL could not be determined. However, the results provided in Tables 5 and 6 are, in the authors' opinion, a valuable aid for the veterinary radiologist in characterising FLL in dogs, as they indicate several qualitative and quantitative CT features that might be useful in differentiating between malignant and benign lesions. However, the diagnostic accuracy of even the most discriminating CT features was only moderate such that aspirate cytology and, in some cases, biopsy histopathology remain necessary to accurately characterise FLL. Nonetheless, informative CT features can lend weight to the results of pathology and provide a more

Table 6
Summary of meta-analysis for quantitative features.

CT feature	Studies (*n*)	Standardized mean difference	SE	*t*	*P*-value
Maximum dimension	4	0.858	0.35	2.44	0.015
Ellipsoid volume	2	0.567	0.28	2.97	0.003
Attenuation of pre-contrast normal liver	4	−0.596	0.30	−2.00	0.046
Attenuation of pre-contrast lesion	3	−0.988	0.52	−1.88	0.062
Attenuation of arterial phase normal liver	3	−0.209	0.16	−1.34	0.183
Attenuation of arterial phase lesion	3	−0.517	0.16	−3.26	0.001
Attenuation of portal phase normal liver	3	−0.057	0.35	−0.16	0.869
Attenuation of portal phase lesion	3	−0.526	0.16	−3.31	0.001
Attenuation of delayed phase normal liver	3	−0.107	0.16	−0.68	0.497
Attenuation of delayed phase lesion	5	−0.377	0.13	−2.98	0.003

SE, standard error; t, Student's t-test.

accurate evaluation of FLL in dogs, while some FLL are located at sites inaccessible to sampling.

Another aspect that emerged from this meta-analysis was the relatively low number of studies (and cases) available in the veterinary literature on this topic, especially when compared to the human literature. The CT features of only 419 FLL in dogs had been described, whereas meta-analyses including thousands of patients are currently available in the medical literature (Lee et al., 2015; Roberts et al., 2018). Such a dissimilarity is, most likely, related to differences in the standards of care between humans and dogs both in access to CT imaging and to subsequent investigation of FLL identified. It is anticipated that, as the number of CT scanners available in veterinary clinics increases, a higher number of cases and FLL will be available for review.

A limitation of this meta-analysis was related to the different scanning protocols used in the included studies. Burti et al. (2021) and Jones et al. (2016) used a dual-phase CT scanning protocol that included only a delayed phase post-contrast scan, while the remaining studies used a triple-phase CT scanning protocol that included arterial, portal, and delayed phase post-contrast scans. Most of the CT features that were deemed informative from the meta-analysis results can be evaluated using either CT scanning protocol. Both heterogeneity and attenuation were informative in all phases, and the remaining informative CT features (i.e. well-defined margins, presence of a capsule, lymph nodes, and maximum dimension) could be evaluated independent of the scanning protocol. Due to the limited number of included studies, a subgroup analysis was not performed.

A low risk of bias was attributed to most of the considered studies. While this indicated an acceptable quality of the veterinary literature on this topic, it did highlight some frequently encountered limitations. For example, none of the authors specified whether the pathologists performing the cytological or histopathological analyses were blinded to the results of the CT imaging. It is suspected that the pathologists had not be blinded, as many of the studies were retrospective and during routine clinical practice there is constant dialogue between radiologists and pathologists, as this is considered to enhance diagnostic accuracy (Raab et al., 2000). The retrospective nature of many of the studies may also have of rendered subsequent blinded review of the cytological or histopathological samples unfeasible. The risk of bias for case selection was considered as high in two studies, Taniura et al. (2009) and Kutara et al. (2014), as they limited their inclusion criteria to only certain FLL histotypes. Neither paper provided justification for such a choice, and therefore a selection bias was evident. The inclusion of data from these studies might have influenced the overall results of the meta-analysis towards an increased pooled diagnostic accuracy for some of the CT features. It is warranted that future studies on this topic should adopt study designs that avoid selection bias.

None of the studies included a power analysis or equivalent estimation method. A lack of effectiveness in study design, as previously highlighted by Di Girolamo and Reynders (2016), is a general problem in the veterinary medical literature. Low incidence rates of primary hepatic neoplasms in dogs (Marolf, 2017), along with the increasing publication pressure exerted on researchers, make such a topic attractive for retrospective, rather than prospective, study.

Because HCC is the most common histotype of FLL in humans and is the liver neoplasia with the most available treatment options (Lee et al., 2015), the medical literature on FLL is mainly focused on the detection and grading of HCC. A continuously updating, extensive and detailed algorithm for the imaging, reporting, and care of HCC in humans, the Liver Imaging Reporting and Data System (LI-RADS; Elsayes et al., 2017) contains guidelines for the use of various diagnostic imaging modalities, including CT, in the surveillance and grading of HCC. In humans, HCC mainly arise in cirrhotic livers, while the correlation between hepatic degenerative disease and HCC has not yet been demonstrated in dogs. The efficacy of some treatments for HCCs have been studied in dogs (Marconato et al., 2020), while treatments for the other liver malignancies have been scarcely described. A veterinary counterpart of the human LI-RADS is currently not available, in part due to a lack of meta-analyses on this topic. Due to the relatively low number of studies available in the literature, the specific CT features of HCC in dogs could not be evaluated separately to those of other malignant FLL in the present meta-analysis. However, increasing numbers of publications focusing on the description of the diagnostic imaging features of FLL in dogs have become available in the last few years. In particular, the ultrasonographic (Warren-Smith et al., 2012), contrast-enhanced ultrasonographic (Nakamura et al., 2010; Morishita et al., 2017; Banzato et al., 2019; Burti et al., 2020), CT, and MRI (Constant et al., 2016; Borusewicz et al., 2019) features of FLL (including HCC) have been described. The data reported in the present study point towards the possible creation of diagnostic algorithms for the diagnosis and management of FLL in dogs.

Most of the meta-analyses on FLL in the human medical literature focus on the relative diagnostic accuracy of MRI and CT in the detection of HCC (Lee et al., 2015; Roberts et al., 2018). A comparison of the diagnostic accuracy of MRI and CT in differentiating between benign and malignant FLL in dogs is not feasible at the present time, as the MRI features of FLL in dogs have rarely been evaluated (Constant et al., 2016; Borusewicz et al., 2019). The low number of publications on this topic is, most likely, related to the limited availability of high-field MRI scanners in the veterinary sector and their limited use in evaluating the abdomen.

A final limitation of the present meta-analysis is that techniques to account for the non-independence of sensitivity and specificity, such as bivariate models and hierarchical summary ROCS could not be performed due to the low number of studies that fit the inclusion criteria (Harbord et al., 2007). Additional studies on this topic are required to remedy this.

Conclusions

The qualitative and quantitative CT features to differentiate malignant from benign FLL were analysed. Well-defined margins, presence of a capsule, abnormal lymph nodes, heterogeneity in the arterial, portal, and delayed phase, maximum dimension, ellipsoid volume, attenuation

Maximum Dimension (cm)

Study	Malignant Total	Mean	SD	Benign Total	Mean	SD	SMD	95%CI	Weight
Burti et al., 2021	32	6.39	4.72	37	4.48	3.87	0.44	[-0.0; 0.9]	26.8%
Leela-Arporn et al., 2019	52	6.60	3.10	18	3.10	1.40	1.25	[0.7; 1.8]	25.4%
Jones et al., 2016	14	6.10	17.00	10	6.00	7.82	0.01	[-0.8; 0.8]	21.6%
Taniura et al., 2009	36	6.78	3.53	40	2.74	0.59	1.62	[1.1; 2.1]	26.2%
Random effects model	**134**			**105**			**0.86**	**[0.2; 1.6]**	**100.0%**

Heterogeneity: $I^2 = 82\%$, $\tau^2 = 0.40$, $p < 0.01$

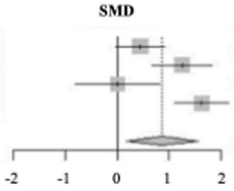

Ellipsoid Volume (cm^3)

Study	Malignant Total	Mean	SD	Benign Total	Mean	SD	SMD	95%CI	Weight
Burti et al., 2021	32	222.90	380.91	37	111.21	343.89	0.31	[-0.2; 0.8]	53.3%
Leela-Arporn et al., 2019	52	195.00	226.60	18	21.30	24.50	0.87	[0.3; 1.4]	46.7%
Random effects model	**84**			**55**			**0.57**	**[0.0; 1.1]**	**100.0%**

Heterogeneity: $I^2 = 57\%$, $\chi^2_1 = 2.31$ ($p = 0.13$)

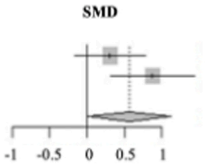

Attenuation of pre-contrast normal liver (HU)

Study	Malignant Total	Mean	SD	Benign Total	Mean	SD	SMD	95%CI	Weight
Stehlik et al., 2021	14	63.10	9.02	17	60.90	8.69	0.24	[-0.5; 1.0]	23.4%
Burti et al., 2021	32	59.39	8.32	37	65.26	7.99	-0.71	[-1.2; -0.2]	28.9%
Jones et al., 2016	14	60.00	5.50	10	71.00	7.50	-1.66	[-2.6; -0.7]	18.1%
Taniura et al., 2009	36	58.10	11.20	40	62.70	8.10	-0.47	[-0.9; 0.0]	29.7%
Random effects model	**96**			**104**			**-0.59**	**[-1.2; 0.0]**	**100.0%**

Heterogeneity: $I^2 = 71\%$, $\tau^2 = 0.23$, $p = 0.02$

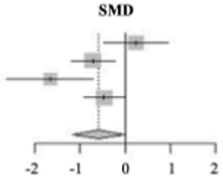

Attenuation of lesion in arterial phase (HU)

Study	Malignant Total	Mean	SD	Benign Total	Mean	SD	SMD	95%CI	Weight
Stehlik et al., 2021	14	52.80	17.24	17	65.00	28.80	-0.49	[-1.2; 0.2]	19.2%
Leela-Arporn et al., 2019	52	112.00	49.60	18	134.70	72.30	-0.40	[-0.9; 0.1]	34.1%
Taniura et al., 2009	36	91.10	35.20	40	116.10	44.40	-0.61	[-1.1; -0.2]	46.7%
Random effects model	**102**			**75**			**-0.52**	**[-0.8; -0.2]**	**100.0%**

Heterogeneity: $I^2 = 0\%$, $\tau^2 = 0$, $p = 0.84$

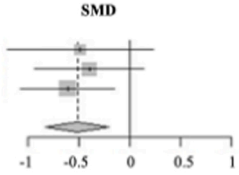

Attenuation of lesion in portal phase (HU)

Study	Malignant Total	Mean	SD	Benign Total	Mean	SD	SMD	95%CI	Weight
Stehlik et al., 2021	14	87.00	30.20	17	83.20	29.28	0.12	[-0.6; 0.8]	12.6%
Burti et al., 2021	32	89.62	40.60	37	90.13	41.96	-0.01	[-0.5; 0.5]	28.2%
Leela-Arporn et al., 2019	52	105.20	28.10	18	119.70	37.50	-0.47	[-1.0; 0.1]	21.5%
Jones et al., 2016	14	77.00	19.50	10	99.00	24.00	-0.99	[-1.9; -0.1]	8.4%
Taniura et al., 2009	36	104.90	34.60	40	123.90	17.50	-0.70	[-1.2; -0.2]	29.3%
Random effects model	**148**			**122**			**-0.38**	**[-0.6; -0.1]**	**100.0%**

Heterogeneity: $I^2 = 50\%$, $\tau^2 = 0.09$, $p = 0.09$

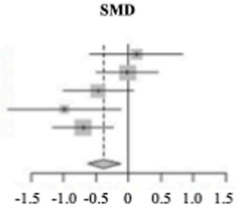

Attenuation of lesion in delayed phase (HU)

Study	Malignant Total	Mean	SD	Benign Total	Mean	SD	SMD	95%CI	Weight
Stehlik et al., 2021	14	87.00	30.20	17	83.20	29.28	0.12	[-0.6; 0.8]	12.6%
Burti et al., 2021	32	89.62	40.60	37	90.13	41.96	-0.01	[-0.5; 0.5]	28.2%
Leela-Arporn et al., 2019	52	105.20	28.10	18	119.70	37.50	-0.47	[-1.0; 0.1]	21.5%
Jones et al., 2016	14	77.00	19.50	10	99.00	24.00	-0.99	[-1.9; -0.1]	8.4%
Taniura et al., 2009	36	104.90	34.60	40	123.90	17.50	-0.70	[-1.2; -0.2]	29.3%
				122			**-0.38**	**[-0.6; -0.1]**	**100.0%**

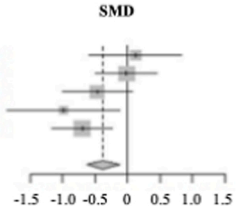

Fig. 3. Pooled standardised mean difference (SMD) for maximum dimensions, ellipsoid volume, attenuation of pre-contrast normal liver, and attenuation of lesion in arterial, portal, and delayed phase post-contrast. 95% CI, 95% confidence interval; SD, standard deviation; HU, Hounsfield unit.

of the liver in the pre-contrast phase, and attenuation of the liver in the arterial, portal, and delayed phase were found to be informative.

Conflict of interest

None of the authors has any other financial or personal relationships that could inappropriately influence or bias the content of the paper.

Acknowledgements

The present paper is part of a project funded by a research grant from the Department of Animal Medicine, Production and Health – MAPS, University of Padua, Italy: SID- Zotti 2018 (€ 32,000; Application of deep-learning algorithms in pet animal diagnostic imaging).

Appendix A. Supplementary data

Supplementary material related to this article can be found, in the online version, at doi:https://doi.org/10.1016/j.tvjl.2021.105773.

References

Ariff, B., Lloyd, C.R., Khan, S., Shariff, M., Thillainayagan, A.V., Bansi, D.S., Khan, S.A., Taylor-Robinson, S.D., Lim, A.K.P., 2009. Imaging of liver cancer. World Journal of Gastroenterology 15, 1289–1300.

Banzato, T., Rubini, G., Orlandi, R., Bargellini, P., Bonsembiante, F., Zotti, A., 2019. Contrast enhanced ultrasound fetaures of hepatocellular carcinoma in dogs. Veterinary Record 186, 187.

Borusewicz, P., Stańczyk, E., Kubiak, K., Spuzak, J., Glińska-Suchocka, K., Jankowski, M., Sławuta, P., Kubiak-Nowak, D., Podgórski, P., 2019. Magnetic resonance imaging of liver tumors using gadoxetic acid (Gd-EOB-DTPA) - Pilot study. BMC Veterinary Research 15, 1–9.

Burti, S., Zotti, A., Rubini, G., Orlandi, R., Bargellini, P., Bonsembiante, F., Banzato, T., 2020. Contrast-enhanced ultrasound features of malignant focal liver masses in dogs. Scientific Reports 10, 1–12.

Burti, S., Zotti, A., Bonsembiante, F., Contiero, B., Banzato, T., 2021. Diagnostic accuracy of delayed phase post contrast computed tomographic images in the diagnosis of focal liver lesions in dogs: 69 cases. Frontiers in Veterinary Science 8, 1–10.

Chou, R., Cuevas, C., Fu, R., Devine, B., Wasson, N., Ginsburg, A., Zakher, B., Pappas, M., Graham, E., Sullivan, S.D., 2015. Imaging techniques for the diagnosis of hepatocellular carcinoma: a systematic review and meta-analysis. Annals of Internal Medicine 162, 697–711.

Constant, C., Hecht, S., Craig, L.E., Lux, C.N., Cannon, C.M., Conklin, G.A., 2016. Gadoxetate disodium (gd-eob-dtpa) contrast enhanced magnetic resonance imaging characteristics of hepatocellular carcinoma in dogs. Veterinary Radiology and Ultrasound 57, 594–600.

DerSimonian, R., Laird, N., 2015. Meta-analysis in clinical trials revisited. Contemporary Clinical Trials 45, 139–145.

Di Girolamo, N., Reynders, R.M., 2016. Deficiencies of effectiveness of intervention studies in veterinary medicine: a cross-sectional survey of ten leading veterinary and medical journals. PeerJ 2016, 1–22.

Elsayes, K.M., Kielar, A.Z., Agrons, M.M., Szklaruk, J., Tang, A., Bashir, M.R., Mitchell, D. G., Do, R.K., Fowler, K.J., Chernyak, V., et al., 2017. Liver imaging reporting and data system: an expert consensus statement. Journal of Hepatocellular Carcinoma Volume 4, 29–39.

Fukushima, K., Kanemoto, H., Ohno, K., Takahashi, M., Nakashima, K., Fujino, Y., Uchida, K., Fujiwara, R., Nishimura, R., Tsujimoto, H., 2012. CT characteristics of primary hepatic mass lesions in dogs. Veterinary Radiology and Ultrasound 53, 252–257.

Griebie, E.R., David, F.H., Ober, C.P., Feeney, D.A., Anderson, K.L., Wuenschmann, A., Jessen, C.R., 2017. Evaluation of canine hepatic masses by use of triphasic computed tomography and B-mode, color flow, power, and pulsed-wave Doppler ultrasonography and correlation with histopathologic classification. American Journal of Veterinary Research 78, 1273–1283.

Harbord, R.M., Deeks, J.J., Egger, M., Whiting, P., Sterne, J.C., 2007. A unification of models for meta-analysis of diagnostic accuracy studies. Biostatistics 8, 239–251.

Higgins, J.P.T., 2003. Measuring inconsistency in meta-analyses. British Medical Journal 327, 557–560.

Jones, I.D., Lamb, C.R., Drees, R., Priestnall, S.L., Mantis, P., 2016. Associations between dual-phase computed tomography features and histopathologic diagnoses in 52 dogs with hepatic or splenic masses. Veterinary Radiolology and Ultrasound 57, 144–153.

Kutara, K., Seki, M., Ishikawa, C., Sakai, M., Kagawa, Y., Iida, G., Ishigaki, K., Teshima, K., Edamura, K., Nakayama, T., et al., 2014. Triple-phase helical computed tomography in dogs with hepatic masses. Veterinary Radiology and Ultrasound 55, 7–15.

Lee, Y.J., Lee, J.M., Lee, J.S., Lee, H.Y., Park, B.H., Kim, Y.H., Han, J.K., Choi, B.I., 2015. Hepatocellular carcinoma: diagnostic performance of multidetector CT and MR imaging-a systematic review and meta-analysis. Radiology 275, 97–109.

Leela-Arporn, R., Hiroshi, O., Genya, S., Kiwamu, H., Tatsuyuki, O., Keitaro, M., Noboru, S., Mitsuyoshi, T., 2019. Computed tomographic features for differentiating benign from malignant liver lesions in dogs. Journal of Veterinary Medical Science 81 (12), 1697–1704.

Marconato, L., Sabattini, S., Marisi, G., Rossi, F., Leone, V.F., Casadei-Gardini, A., 2020. Sorafenib for the treatment of unresectable hepatocellular carcinoma: preliminary toxicity and activity data in dogs. Cancers 12, 1272.

Marolf, A.J., 2017. Diagnostic imaging of the hepatobiliary system: an update. Veterinary Clinics of North America - Small Animal Practice 47, 555–568.

Methley, A.M., Campbell, S., Chew-Graham, C., McNally, R., Cheraghi-Sohi, S., 2014. PICO, PICOS and SPIDER: a comparison study of specificity and sensitivity in three search tools for qualitative systematic reviews. BMC Health Service Reserch 14.

Moher, D., Liberati, A., Tetzlaff, J., Altman, D.G., Altman, D., Antes, G., Atkins, D., Barbour, V., Barrowman, N., Berlin, J.A., et al., 2009. Preferred reporting items for systematic reviews and meta-analyses: the PRISMA statement. PLoS Medicine 6.

Morishita, K., Hiramoto, A., Michishita, A., Takagi, S., Osuga, T., Lim, S.Y., Nakamura, K., Sasaki, N., Ohta, H., Takiguchi, M., 2017. Washout ratio in the hepatic vein measured by contrast-enhanced ultrasonography to distinguish between inflammatory and noninflammatory hepatic disorders in dogs. Journal of Veterinary Internal Medicine 31, 770–777.

Nakamura, K., Takagi, S., Sasaki, N., Bandula Kumara, W.R., Murakami, M., Ohta, H., Yamasaki, M., Takiguchi, M., 2010. Contrast-enhanced ultrasonography for characterization of canine focal liver lesions. Veterinary Radiology and Ultrasound 51, 79–85.

Raab, S.S., Oweity, T., Hughes, J.H., Salomao, D.R., Kelley, C.M., Flynn, C.M., D'Antonio, J.A., Cohen, M.B., 2000. Effect of clinical history on diagnostic accuracy in the cytologic interpretation of bronchial brush specimens. American Journal of Clinical Pathology 114, 78–83.

Roberts, L.R., Sirlin, C.B., Zaiem, F., Almasri, J., Prokop, L.J., Heimbach, J.K., Murad, M. H., Mohammed, K., 2018. Imaging for the diagnosis of hepatocellular carcinoma: a systematic review and meta-analysis. Hepatology 67, 401–421.

Shah, S., Shukla, A., Paunipagar, B., 2014. Radiological features of hepatocellular carcinoma. Journal of Clinical and Experimental Hepatology 4, S63–S66.

Shim, S.R., Kim, S.J., Lee, J., Rücker, G., 2019. Network meta-analysis: application and practice using R software. Epidemiological Health 4.

Stehlík, L., Di Tommaso, M., Del Signore, F., Paninárová, M., Terragni, R., Magni, T., Pontonutti, L., Carloni, A., Alberti, M., De Magistris, A.V., et al., 2020. Triple-phase multidetector computed tomography in distinguishing canine hepatic lesions. Animals 11, 11.

Taniura, T., Marukawa, K., Yamada, K., Hikasa, Y., Ito, K., 2009. Differential diagnosis of hepatic tumor-like lesions in dog by using dynamic CT scanning. Hiroshima Journal of Medical Science 58, 17–24.

Warren-Smith, C.M.R., Andrew, S., Mantis, P., Lamb, C.R., 2012. Lack of associations between ultrasonographic appearance of parenchymal lesions of the canine liver and histological diagnosis. Journal of Small Animal Practice 53, 168–173.

Whiting, P.F., Rutjes, A.W., Westwood, M.E., Mallett, S., Deeks, J.J., Reitsma, J.B., Leeflang, M.M., Sterne, J.A., Bossuyt, P.M., 2011. QUADAS-2 Group. QUADAS-2: a revised tool for the quality assessment of diagnostic accuracy studies. Annals of Internal Medicine 155, 529–536.